Original Article

Institution of MECHANICAL ENGINEERS
Journal of ENGINEERING IN MEDICINE

Proc IMechE Part H:
J Engineering in Medicine
2017, Vol. 231(12) 1213–1223

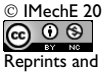
Reprints and permissions:
sagepub.co.uk/journalsPermissions.nav
DOI: 10.1177/0954411917740388
journals.sagepub.com/home/pih


The Memo*Slide*: An explorative study into a novel mechanical follow-the-leader mechanism

Paul WJ Henselmans, Stefan Gottenbos, Gerwin Smit and Paul Breedveld

Abstract

Follow-the-leader propagation allows for the insertion of flexible surgical instruments along curved paths, reducing the access required for natural orifice transluminal endoscopic surgery. Currently, the most promising follow-the-leader instruments use the alternating memory method containing two mechanical memory-banks for controlling the motion of the flexible shaft, which reduces the number of actuators to a minimum. These instruments do, however, require concentric structures inside the shaft, limiting its miniaturization. The goal of this research was, therefore, to develop a mechanism conforming the principles of the alternating memory method that could be located at the controller-side instead of inside the shaft of the instrument, which is positioned outside the patient and is therefore less restricted in size. First, the three-dimensional motion of the shaft was decoupled into movement in a horizontal and vertical plane, which allowed for a relatively simple planar alternating memory mechanism design for controlling planar follow-the-leader motion. Next, the planar movement of the alternating memory mechanism was discretized, increasing its resilience to errors. The resulting alternating memory mechanism was incorporated and tested in a proof-of-concept prototype called the Memo*Slide*. This prototype does not include a flexible shaft, but was fully focused on proving the function of the alternating memory mechanism. Evaluation of the Memo*Slide* shows the mechanism to work very well, being able to transfer any planar path that lays within its physical boundaries along the body of the mechanism without accumulating errors.

Keywords

Natural orifices transluminal endoscopic surgery, minimally invasive surgery, surgical instruments, follow-the-leader, pathway surgery

Date received: 5 April 2017; accepted: 11 October 2017

Introduction

Advancements in minimally invasive surgery (MIS) have led to a reduction in the invasiveness of surgical procedures, leading to less scar tissue, a lower risk of infection, and shorter hospital stays.[1–3] The field of natural orifices transluminal endoscopic surgery (NOTES) strives to further reduce the negative effects of surgery using natural orifices such as the mouth, nose, and anus as the surgical entry point.[4,5] This approach does introduce technical challenges as the currently used rigid Ø5-mm instruments designed for MIS are not able to confine to the curved nature of the human anatomy but dictate a straight path from entry point to lesion. Making the Ø5-mm instruments flexible, as for example the MultiFlex of Figure 1(a), could therefore extend the reach of NOTES procedures in compact anatomical areas.[6,7]

In order to maneuver a flexible instrument through compact anatomical areas, its movements must be controlled in such a manner that the instrument propagates along a curved path, comparable to the motion of a biological snake. A snake steers its head while the remainder of its body follows the created path. In this way, the snake is able to navigate through cluttered environments while avoiding obstacles like the stones in Figure 1(b). Chose et al. introduced the term follow-the-leader (FTL) for this type of movement as the

Department of BioMechanical Engineering, Delft University of Technology, Delft, The Netherlands

Corresponding author:
Paul WJ Henselmans, Department of BioMechanical Engineering, Delft University of Technology, Mekelweg 2, 2628 CD Delft, The Netherlands.
Email: p.w.j.henselmans@tudelft.nl

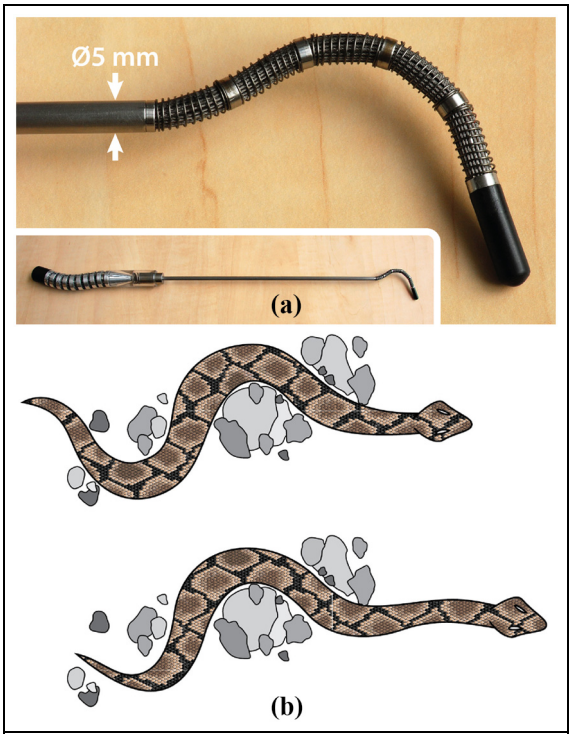

Figure 1. Flexible surgical instrument and follow-the-leader propagation. (a) The MultiFlex, an Ø5-mm flexible instrument with 10 degrees of freedom.[8] The instrument is controlled by manually adjusting the shape of the handle, which is mimicked by the flexible part of the shaft. (b) Snake moving through a cluttered environment by transferring a curved path initiated by its head along its body. This motion is referred to a follow-the-leader propagation.

snake's body follows the head that functions as the leader.

In the following section, the state of the art in FTL instruments will be discussed based on the used technique and its potential for miniaturization to Ø5 mm. Techniques that require interaction with the environments in order to propagate along a curved path, for example, a catheter that is guided through a lumen, are not considered. Only techniques that are able to move in free space without guidance from the environment are regarded as FTL instruments and will be discussed.

State of the art

Concentric tube robots are currently the thinnest existing instruments mentioned in research toward FTL propagation.[9–12] These instruments contain a telescoping mechanism of pre-curved compliant tubes placed concentrically within one another. Rotating or translating the tubes relative to each other causes them to interact and deform, with the result that the instrument changes shape. Based on a model of the interaction between the tubes, a control sequence can be planned in order to achieve FTL propagation.[13,14] However, the pre-defined curvature and compliancy of the tubes restrict the propagation to only specific and relatively simple paths, like a single bend or a constant curvature helix, that have to be planned prior to the surgical procedure.

A number of FTL instruments that can follow non-specific paths without planning were also found in the literature. Typically, their shafts contain multiple degrees of freedom (DOF) that are independently controlled by an individual actuator.[15–23] These actuators can be embedded in the shaft near the DOF they actuate.[15–19] Embedding the actuators within an Ø5 mm shaft is highly challenging while maintaining sufficient power output at safe temperatures. With the addition of a transmission system, the actuators can also be placed outside of the shaft at the controller-side of the instrument, for example, using cables that connect the actuator placed outside the shaft to the DOF in the shaft.[20–22] Actuators placed at the instrument's controller-side, and therefore outside the patient, are less restricted in size. The thinnest instrument found in the literature using this approach is Ø8 mm. Its shaft consists of three telescoping segments that each can be bend in 2 DOFs using cables. In principle, these instruments could be miniaturized down to Ø5 mm.[20,21] Moreover, by connecting each DOF to an individual actuator, the DOF can be independently controlled which allows for propagation along non-specific paths without the need for planning.

A downside of using an individual actuator for every DOF in the shaft is that it requires a large number of actuators. Moreover, as a complex three-dimensional (3D) path requires more DOF in the shaft than a path with a single curve, the complexity of the path that can be followed becomes dependent on the number of actuators in the system. As medical-grade actuators (conforming to ISO 13485) are not cheap, for example, a DC motor with gearhead can easily cost over € 200, and it is preferable to use a minimal number of actuators.[24]

There are instruments capable of propagating along tortuous paths with less than one actuator for each DOF.[25–27] The most promising instrument is the highly articulated robotic probe (HARP), which consists of two concentrically placed arms that contain friction-based locking systems to switch between rigid and flexible states (Figure 2(a)).[26,27] FTL propagation is achieved by a series of alternating steps. First, the inner arm is rigidified, while the outer arm is made flexible. The outer arm is then advanced forward while using cables to steer its tip in the desired direction (Figure 2(b)). Next, the outer arm is rigidified, while the inner arm is made flexible (Figure 2(c)). The inner arm is now advanced forward while being guided by the rigid outer arm (Figure 2(d)). Once the inner arm catches up with the outer arm, the sequence is repeated. The HARP therefore only needs actuators for steering, rigidifying and advancing its arms, with the result that the complexity of the path becomes independent from the number of actuators.

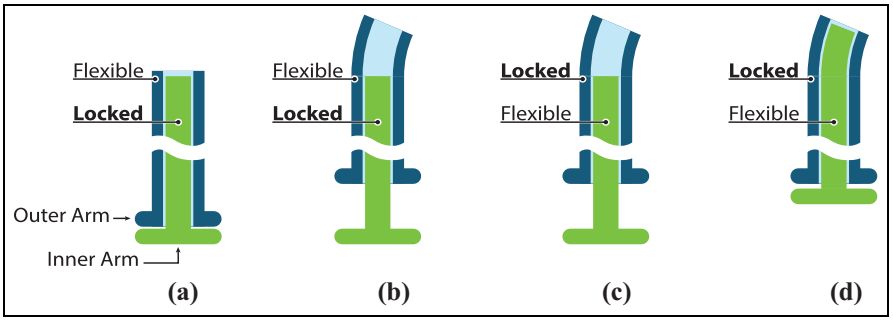

Figure 2. Schematic 2D drawing showing the functioning of the HARP consisting of two concentrically placed flexible arms which can both be independently locked.[26,27] (a) Inner-arm locked and outer-arm made flexible, (b) Flexible outer-arm advanced forward while steering, (c) Outer-arm locked and inner-arm made flexible, (d) Inner-arm catches up with outer-arm. For explanation, see text.

The HARP's outer diameter is 12 mm and is difficult to miniaturize down to the desired Ø5 mm due to its concentrically placed friction-based locking systems. The locking systems are build out of a series of ball-joints, which can be pressed together via cables to induce friction creating a friction torque around the joints and therefore rigidifying the shaft. Miniaturization of the shaft's diameter with a scaling factor of s reduces the moment arm of the friction torque with factor s, therefore increasing the required friction force by the same factor s. Moreover, the surface area of the friction force will decrease with factor s^2. The increase in friction force and decrease in surface area will cause the material stress to increase with factor s^3, making it very difficult to avoid plastic deformation. The HARP's method of FTL propagation is, however, very interesting: where normally the path information is measured and memorized by a computer that drives a set of actuators, one for each DOF, the HARP is based on two mechanical memory-banks (the two concentric arms) that alternate between copying, memorizing, and shifting the path information. The result is that the complexity of the path becomes independent from the number of actuators. In this article, this method for FTL propagation will be referred to as the "Alternating Memory method" or AM method.

Problem statement and goal

An instrument using the AM method for FTL propagation alternates the path information between two mechanical memory-banks. The advantage is that the instrument does not require an actuator for every degree of freedom (DOF) in its flexible shaft, with the result that the number of actuators is fixed and becomes independent of the complexity of the path. Placing the memory-banks inside the instrument's flexible shaft does, however, impede miniaturization of the shaft, as seen in the HARP. In this article, we introduce a novel concept using the AM method for FTL propagation, while focusing on the development of a control mechanism that can be located at the controller-side of the instrument, which is outside of the patient and therefore less restricted in size.

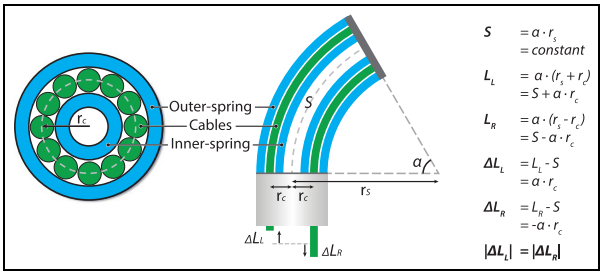

Figure 3. Cable-ring mechanism. Left: schematic cross-sectional view of a cable-ring mechanism. Cables are enclosed in a ring by an inner-spring and an outer-spring. Right: schematic side view of a cable-ring segment in bent position. Assuming that the centerline (S) does not change length, the absolute length change ($|\Delta L|$) of antagonist cables is equal.

Mechanism design

Miniaturization of the shaft with the cable-ring mechanism

If the memory-banks are placed at the controller-side of the instrument, then the motions of its memory-banks have to be transported toward the flexible shaft. This can be realized by the cable-ring mechanism in which a set of steering cables is enclosed in a ring between two springs as illustrated in Figure 3.[28]

By fixing cables at intermediate points along the length of the shaft, the maneuverability of the shaft is enhanced. The MultiFlex of Figure 1(a) is an example of a cable-ring controlling five segments with a total of 10 DOFs within a Ø5 mm shaft.[8] The elegance of this mechanism is that the cables keep each other aligned, which eliminates the need for additional guiding components while maximizing the number of cables. The number of cables in a cable-ring can be calculated by

$$n_{cables} = \frac{2 \cdot \pi \cdot r_c}{d_{cable}} \quad (1)$$

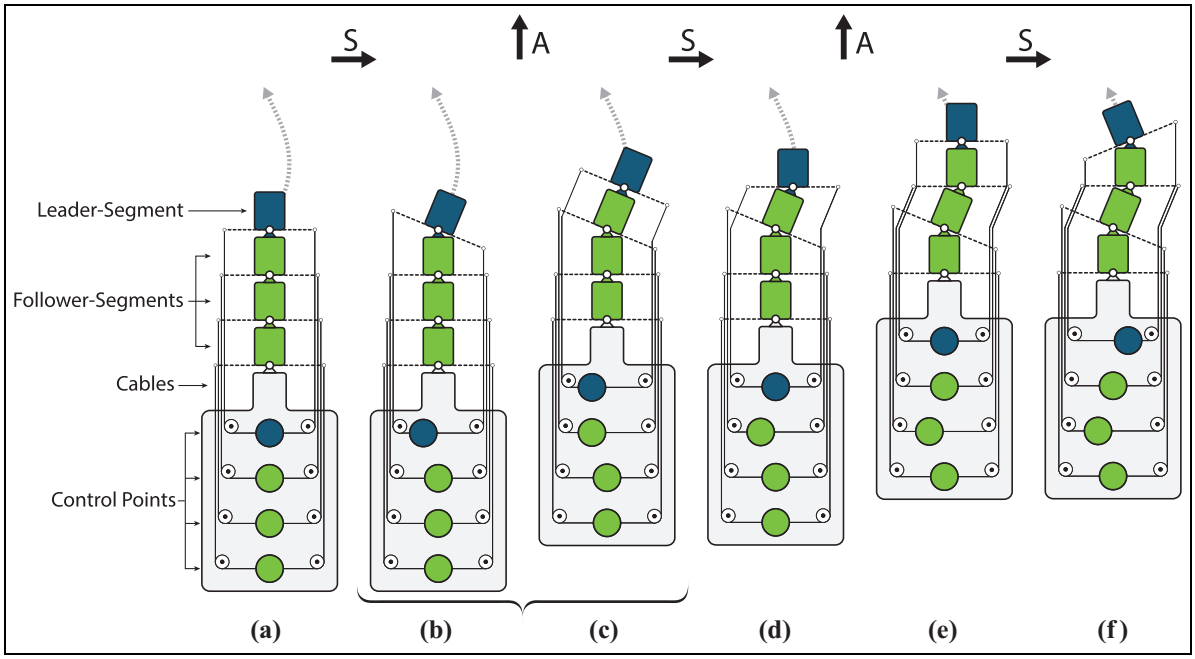

Figure 4. Two-dimensional schematic representation of cable control for follow-the-leader (FTL) propagation. Arrows with an "S" stand for a steering action. Arrows with an "A" stand for an advancing action. Labels (a) to (f) inclusive indicate a sequence of configurations, which are further explained in the text. The brace is used in Figure 5.

where r_c (mm) is the radius of the cable-ring and d_{cable} (mm) the diameter of the cables. For a Ø5-mm shaft design including Ø0.2 mm stranded steel cables and an outer-spring with Ø0.2 mm wire, the maximum radius of the cable-ring will be 2.3 mm. This allows for approximately 72 cables. Using four cables to control each segment in 2 DOFs, this shaft design allows for a maximum of 18 segments with a total of 36 DOFs at a diameter of only Ø5 mm. The cable-ring mechanism thus offers a convenient solution to transport the motions of the memory-banks from the controller-side to shaft, while enabling miniaturization of the shaft to the desired dimensions.

The cables can be guided from the proximal side of the shaft toward the memory-banks using, for example, pulleys, tubes, guiding slots, or Bowden cables. Such guiding methods are commonly applied in steerable instrumentation.[29–31]

The function of the memory-banks is to control the distance over which a cable is pulled or released. Assuming that segment bends with a constant curvature as illustrated on the right of Figure 3, the distance over which a cable travels (ΔL_c, mm) relates to the radius of the cable-ring (r_c, mm) and the bending angle of the segment (α, rad) as

$$|\Delta L_C| = r_c \cdot \alpha \tag{2}$$

Equation (2) shows that in order to reach a bending angle of 100° with the proposed cable ring dimensions, a cable needs to be shifted over ±4 mm. Equation (2) holds for both a cable that is pulled and its antagonist that is released.

Cable control for FTL propagation

A two-dimensional (2D) representation of a shaft connected to the cables of a cable-ring is shown in Figure 4(a). The shaft consists of $N = 4$ segments, the first segment being the leader segment, and the other three segments being the follower segments. At the controller-side of the instrument, the cables controlling the four segments in the shaft are connected to components referred to as control-points. From equation (2), it is clear that the absolute length changes between antagonist cables is equal, consequently antagonist cables can be connected at opposite sides of the same control-point. A sideways translation of a control-point results in a rotation of the connected segment. The configuration of all control-points together determines the overall shape of the shaft.

FTL propagation can be realized by repeating the following two actions as indicated by the arrows in Figure 4. Starting with steering, the direction of the leader segment is changed by translating the first control-point (the leader control-point) sideways (Figure 4(b)). Following with advancing, the instrument is pushed one segment length forward while the steering action given to the first segment is transported along its adjacent segment. This shifting of information also occurs between the other segments, that is, the position of control-point 1 is moved to control-point 2, the position of control-point 2 is moved to control-point 3, and so on (Figure 4(c)). Next, the leader-element is steered to another direction (Figure 4(d)), after which another advancing step is made (Figure 4(e) and (f)). During FTL propagation, the steering and advancing actions are repeated multiple times.

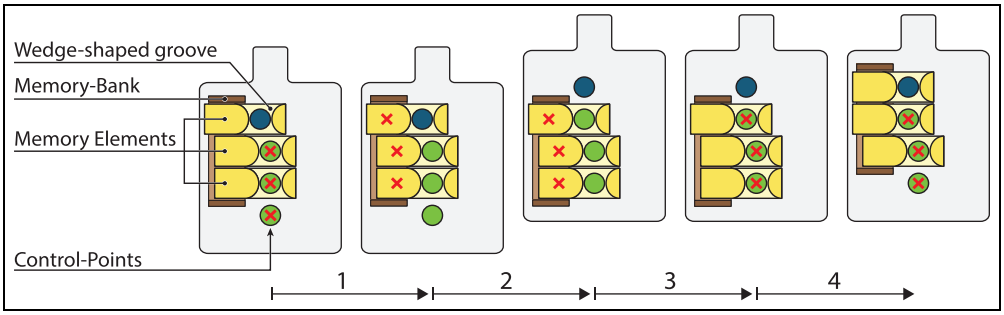

Figure 5. The instrument of Figure 4 drawn without the shaft with the addition of an alternating memory (AM) mechanism. The figure zooms in on the advancing action above the brace of Figure 4. For explanation, see text.

The AM mechanism

For updating the positions of the control-points during the advancing action, a mechanism needs to be added at the controller-side of the instrument in Figure 4. This mechanism must interact with the control-points so that their positions are moved to the adjacent control-points as the instrument moves forward. A mechanism with this functionality is shown in Figure 5 and will be referred to as the AM mechanism. The basic components of the AM mechanism are a memory-bank and a set of memory-elements. The memory-bank encloses the memory-elements and can slide vertically over a distance of one segment. The memory-elements can slide individually from left to right within the memory-bank. They contain wedge-shaped grooves enclosing the control-points that control the segments. These wedge-shape grooves enable the memory-elements to copy the position of a control-point.

The configuration of the memory-elements and the control-points can be memorized by locking them in position. This locking occurs in an alternating fashion, that is, when the control-points are locked, the memory-elements are released, and vice versa. A locked component is visualized in Figure 5 by a cross inside the component, for example, in the left part of Figure 5 the control-points are locked while the memory-elements are released.

Looking at the advancing action for FTL propagation, highlighted by the brace in Figure 4, the functioning of the AM mechanism is based on the following four steps (see arrows in Figure 5):

1. The positions of the memory-elements are locked, after which the control-points are released.
2. The instrument with the control-points is slid one step upward while the memory-bank holds its position. The wedge-shaped grooves in the memory-elements force the control-points to align with the locked memory-elements.
3. The positions of the control-points are locked, after which the memory-elements are released.
4. The memory-bank is slid one step upward to its initial position relative to the instrument. The wedge-shaped grooves of the memory-elements now force the memory-elements to align with the locked control-points, reading out the new position of the control-points.

The mechanism thus alternates between copying, memorizing, and shifting path information by copying and sliding the position of the control-points.

Proof-of-concept prototype

In order to test the AM mechanism of Figure 5, the mechanism was translated into a proof-of-concept (PoC) prototype called Memo*Slide* (Figure 6). The Memo*Slide* was designed to control a shaft with $N = 11$ segments, that is, 1 leader-element and 10 follower-elements. The PoC prototype does not yet include a flexible shaft; its design was purely focused on testing the novel concept of the AM mechanism.

The control-points of the mechanism that were previously unsupported are now supported to leader and follower-elements as shown in Figure 6(a). In the Memo*Slide*, the motion of these elements is constrained so that they can only translate sideways. Above the memory-elements and follower-elements, two locking-bars were added that lock the memory and follower-elements. Two sets of cams, a left set and a right set (Figure 6(c)–(e)), regulate the locking motion as well as the sliding motion of the memory-bank. Operating the mechanism is realized by a steering wheel and crank. With the steering wheel, the user can control the steering action of the leader-element. Rotating the crank drives the cam mechanism that sets the advancing action for FTL propagation in motion.

A detailed view of the locking-bars and the cams is given in Figure 6(d) and (e). The bottom part of the two locking-bars is fitted with a row of three teeth, and each of the memory and follower-elements are fitted with an array of similar teeth. Controlled by the cams, the locking-bars are raised or dropped, interlocking their teeth with those of the memory or follower-elements, respectively, resulting in releasing and locking of the corresponding elements.

The cams regulate the four steps of the AM mechanism, represented by the up/down motion of the

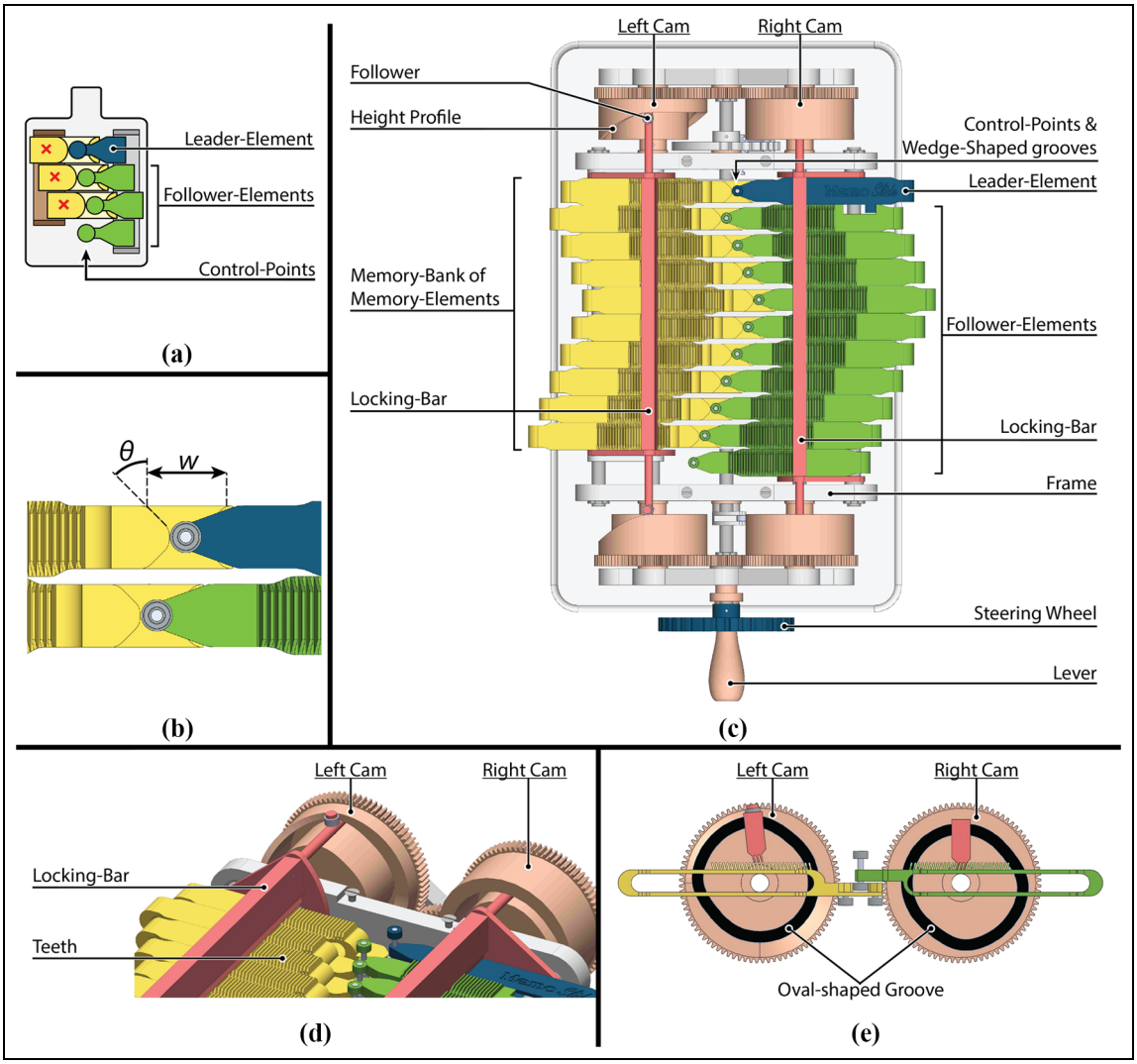

Figure 6. The proof-of-concept prototype Memo*Slide*: (a) schematic representation with the control-point now supported by the leader and follower-elements. (b) Close-up of the control-points and wedge-shaped grooves in the Memo*Slide*. (c) Top view of the Memo*Slide* showing all its components. The steering wheel is used for the steering action of Figure 4, moving the leader-element to the left of right. The crank is used for the advancing action of Figure 4, rotating the cams that regulate the locking of the elements and the sliding motion of the memory-bank. The sliding motion of the memory-bank is initiated by the height profile on the circumference of the left cam pushes the left locking-bar downward. (d) 3D View of the cam-driven discrete locking system. (e) The oval-shaped grooves in the cams regulate the lowering and raising of the locking-bars, respectively, resulting in the locking and releasing of the corresponding elements.

locking-bars and the forward/backward sliding motion of the memory-bank. Locking and releasing the locking-bars is realized by connecting the bars to horizontal rods that slide in oval-shaped grooves within the cams (Figure 6(e)). Rotating the two cams results in the required up/down motion of the bars, in a way that the two bars are out of phase, so that a simultaneous rotation of both cams will result in the alternative locking and releasing of the follower and memory-elements as shown in steps 1 and 3 of Figure 5.

The range and discrete step-size of the steering action, and the range of motion of the entire shaft, are determined by the dimensions of the wedge-shaped groove, the distance between the teeth and the number of teeth, respectively. The dimensions of the wedge-shaped groove are based on its width (w) and angle (θ) (Figure 6(b)). The maximum travel distance of a cable was calculated to be 4 mm. To accommodate left and right steering, the width of the wedge-shaped grooves needs to be at least twice as long and was set at 8 mm. Various wedge angles are possible; for this design, an angle of 45° was chosen based on initial tests to find a good balance between the sliding distance and operation force. In future designs, this angle can be further optimized. The distance between the teeth was chosen to be 1 mm. Using equation (2), each interval translates to a 25° bend of a shaft segment. The number of teeth was set on 31, which means the shaft would be able to bend 375° in both direction starting from its initial straight position.

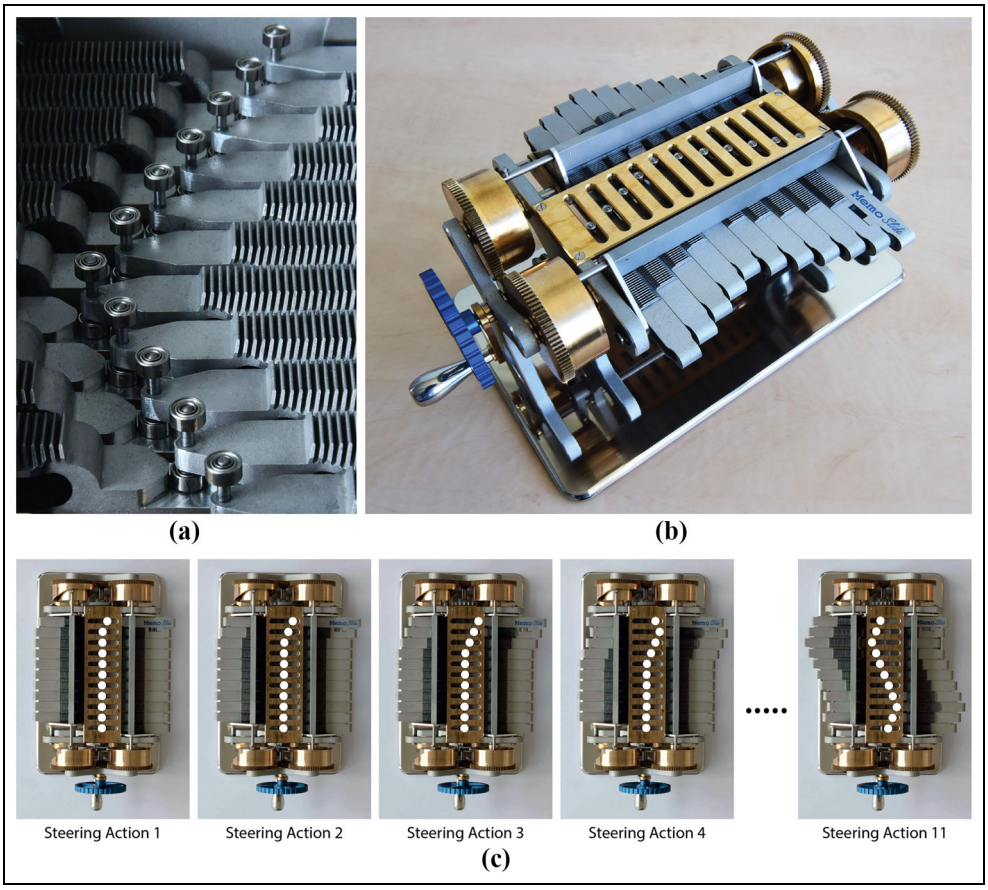

Figure 7. Finished Memo*Slide*: (a) close-up of the interaction between the memory-elements (left) and the follower-elements (right), each follower-element containing two ball-bearings, one at the top and one at the bottom, the bottom one interacting with the wedge-shaped grooves. (b) Photo of the entire prototype with the top ball-bearings of the follower-elements guided through slots in a bronze plate and displaying—as an example—a triangular path. (c) Top view of the Memo*Slide* showing a triangular path propagating through the mechanism. A video of the functioning Memo*Slide* can be found alongside the digital version of this article.

The Memo*Slide* was fabricated and is shown in Figure 7. The device has a footprint of 129 mm by 143 mm, about the size of an A5 piece of paper, and a height of 102 mm. The control-points of the mechanism were embodied by a set of ball bearings attached to the bottom of the follower-elements as to realize a smooth interaction with the wedge-shaped grooves of the memory-elements (Figure 7(a)). Another set of ball bearings, attached to the top of the follower-elements, run through slots in a bronze plate shown at the top of the mechanism in Figure 7(b). This plate was added to smoothly guide the sideways motion of the elements. Most components were made out of aluminum, whereas bronze bushings was used for parts involved in sliding contact. The axes that support the cams and steering mechanism were made of stainless steel due to its strength and low friction coefficient with the bronze. The result is that Memo*Slide* operates smoothly with a very low required operating force on the crank.

Functional evaluation

The Memo*Slide* was developed in order to prove the concept of the AM mechanism. As an example, the series of photos in Figure 7(c) show a triangular path that is propagated through the Memo*Slide*. Initially, all follower control-points (denoted by white dots in Figure 7(c)) are aligned at the center of the prototype, which relates to a straight shape of an instrument shaft. The motion starts with a steering action to the right and continues with a series of other steering action creating a triangular path that is transported along the adjacent segments by alternately rotating the steering wheel and rotating the crank. A video of the functioning Memo*Slide* can be found online alongside the digital version of this article.

During the triangular path of Figure 7(c), the torque on the crank was measured to be between 0.875 and 3.5 N/mm. The peak torque was measured during the sliding motion of the memory-banks, while the lowest amount of torque was measured when only the cams were moving and can thus be credited to the friction between the bronze slide bushings of the cam system.

The Memo*Slide* mechanism works in two directions. By turning the crank clockwise, the positions of the control-points propagate downward in Figure 7(c) and by turning the crank counterclockwise the positions of the control-points propagate upward in Figure 7(c).

This reversibility allows for the re-shaping of the shaft by retracting the shaft up to the point where a change of shape is desired. More importantly, it ensures that the instrument's shaft can be retracted along the same path over which it was propagated.

Discussion

The range of the MemoSlide

The elegance of the AM mechanism in the Memo*Slide* is that it can create a large amount of different paths with only steering and advancing actions as input. The number of paths can be calculated by

$$number\ of\ paths = sr^N \tag{3}$$

where sr is the steering range, that is, the number of discrete positions one can choose from during a steering action, and N is the number of elements. The Memo*Slide* includes 11 elements ($N = 11$) and its steering range is equal to 9 discrete steering positions (4 positions of the leader-element to the left, 4 positions of the leader-element to the right, and 1 position in the middle relative to the adjacent follower-element) ($sr = 9$). As a result, Memo*Slide* has the potential to create a total of nine^{12} different paths. In its current design, however, the array of 31 teeth on the elements is not enough to support all these paths. The next paragraph will discuss how the design choices of the AM mechanism affect the functioning and range of motion for a cable-ring actuated shaft.

Design choices

The design choices that mainly affect the functioning of the mechanism are the size of the teeth, the play between interlocked teeth, and the angle of the wedge-shaped grooves. The size of the teeth determines the level of discretization of the steering action. Smaller teeth will increase the level of discretization, but are weaker and more challenging to fabricate. The teeth were fabricated out of high-strength aluminum (Al7075) using electric discharge machining that, as opposed to other machining techniques as milling or sawing, does not create any reaction force on the material preventing the teeth to deform during machining. The interval of the teeth was set on 1 mm, and the teeth were given a thickness of 0.45 mm while the gap between the teeth was set at 0.55 mm. As a result, there is a maximum of 0.1 mm play between interlocked teeth ensuring them to interlock smoothly, yet influencing the precision of the mechanism itself. The play between the teeth could be eliminated by giving the teeth a triangular shape instead of their current rectangular shape.

The overall dimensions of the AM mechanism are mainly dictated by the width of the memory-elements, which is determined by the angle (θ) and width (w) of the wedge-shaped grooves (Figure 6(b)). A larger wedge angle would allow for thinner elements and thus a more compact AM mechanism design, yet also increases the operating force of the AM mechanism. As the AM mechanism is placed outside the patient, its size is less crucial, and smaller wedge angles were therefore chosen for a smoother functioning of the mechanism.

The MemoSlide as a surgical instrument

The schematic representation of Figure 8(a) illustrates how the Memo*Slide*'*s* AM mechanism can be integrated into a functional surgical instrument. The instrument is visualized by a cart, which holds the AM mechanism and flexible shaft and runs over a gear rack that is fixed to the ground (Figure 8(a)). The leader and follower-elements of the AM mechanism will be connected to the segments of the flexible shaft by cables, as illustrated in Figure 4 (cables not drawn in Figure 8(a)). A joystick is connected to the leader-element and used to steer the leader-element (top Figure 8(a)).

The movements of the AM mechanism can be synchronized with the forward and backward movement of the instrument by including two sets of wheels on the cart. One set supports the leader and follower-elements and the shaft and is connected to the corresponding locking mechanism. The other set supports the memory-bank and is also connected to the corresponding locking mechanism. In this way, the shaft can be moved forward or backward when the memory-bank is locked, corresponding to step 2 in Figure 5. When the leader and follower-elements and thus the shape of the shaft is locked, the memory-bank is free to slide back, corresponding to step 4 in Figure 5.

During the advancing step of FTL propagation as illustrated in Figure 4, the shaft is pushed one step forward during which its shape is transformed. This transformation can cause a temporary deviation from the path, especially when the step-size over which the shaft is moved forward or backward is large. In Figure 4, each step was set to be the length of one shaft segment. The forward step-size can, however, also be smaller, for example, a fourth of the segment length. This will require that the cables of the shaft are not connected to every element of the AM mechanism, but to every fourth element. In that case four instead of one element embody the full steering range of a single shaft segment. An advantage is that the difference in position between adjacent element will be smaller, resulting in a more fluent transition between steering steps. A drawback of this approach is the increasing number of elements in the AM mechanism. The effect of the step-size of the advancing step on the path following accuracy will be investigated in future research.

Once integrated into a surgical instrument, the AM mechanism will be subjected to loading caused by tension in the cables. Because antagonist cables are connected to the same element of the AM mechanism as illustrated in Figure 4, an equal pre-tension in antagonist cables will balance out and therefore not cause any

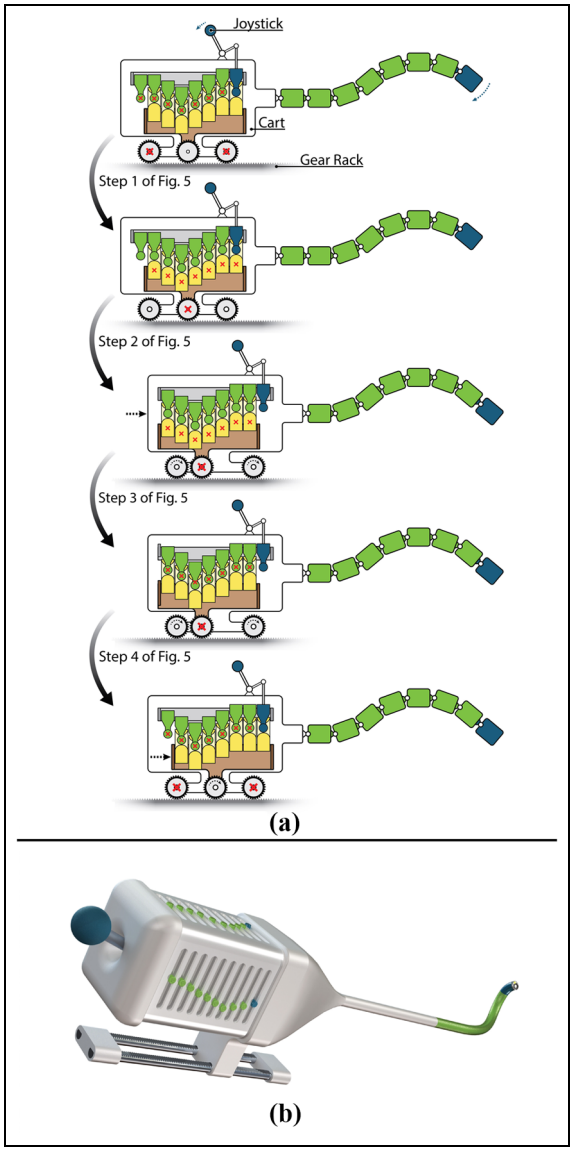

Figure 8. The Memo*Slide* as a surgical instrument: (a) schematic representation of how the AM mechanism can be integrated into an instrument. The AM mechanism and shaft are placed on a cart, which runs over a gear rack that is fixed to the ground. Cables connect the segments of the flexibles shaft to the leader and follower-elements as was illustrated in Figure 4 (cables not drawn). At the top, the leader segment is steered using a joystick. In the middle, the entire instrument is pushed one segment length forward while the memory-bank remains stationary to the ground (illustrated by the cross) and updates the shape of the shaft. At the bottom, the memory-bank slides back and the instrument regains its initial configuration. The transitions between the images represent steps 1–4 of Figure 5. (b) Artistic impression of an instrument capable of follow-the-leader propagation in 3D. Based on the Memo*Slide*, the instrument incorporates two 2D alternating memory (AM) mechanisms that separately control the movements in the vertical and horizontal plane. Steering the instrument is realized by a joystick, which connects to both AM mechanisms.

loading on the AM mechanism. An unequal tension between antagonist cables caused by the weight and bending stiffness of the shaft, or external forces will cause loading of the AM mechanism. When the leader and follower-elements are locked, this load is supported by the locking system and will not affect the functioning of the mechanism. The loading does come apparent during the sliding motion of the locked memory-bank (step 2 in Figure 5). At this point, the follower-elements are momentarily unsupported and uneven tension between antagonist cables may cause them to shift. The range of this shift varies between 0 and 4 mm, depending on the configuration of the mechanism, and the result is an undesired shape change of the unlocked shaft. To prevent this undesired movement, there must be a force present that is higher than the difference in tension between the antagonist cables. The intrinsic friction on the cables and follower-elements might already be sufficient, for example, the shaft of the MultiFlex of Figure 1(a) includes springs, yet remains in any bent position due to the intrinsic friction of the instrument. When the intrinsic friction is not enough, additional friction must be intentionally induced. Intentionally inducing friction will increase the operating force of the AM mechanism, making it only viable for small loads caused by light shafts with low bending stiffness or low external forces. The AM mechanism therefore has the limitation that it cannot handle high loads during FTL propagation without intentionally induced friction, which is a topic for future research. Nevertheless, once the shaft is at rest, its shape is locked and external loading is possible. Moreover, at this point, the leader segment of the shaft is free to be steered for changing the view of the endoscope or for manipulation purposes.

The schematic representation of Figure 8(a) still only functions in a 2D plane, and the next step of this research will therefore be focused on developing an instrument capable of FTL propagation in 3D space. An artistic impression of a 3D FTL instrument is presented in Figure 8(b). As the developed AM mechanism can only control segments in a single plane, two separate AM mechanisms will be incorporated into the design of this instrument. These two AM mechanisms will altogether control the 3D movements of the flexible shaft.

A strong benefit of constructing the 3D mechanism out of two 2D AM mechanisms is that the control over the horizontal and vertical movement, as seen from an individual segment, is fully decoupled. The result is two relatively simple planar mechanisms that function completely independent from one another, that is, an action in one mechanism does not affect the other. This decoupling allows for a design that is fully dedicated to a single function, allowing great freedom for design optimization and precise manufacturing.

Another advantage of using a set of two 2D AM mechanisms is that a 2D mechanism allows easy implementation of a discrete locking system. Although limiting the motion of each DOF to a number of discrete intervals, using discrete locking by means of teeth has an important advantage over using continuous locking

by means of friction. With friction locking, small errors can occur in case of a mismatch between the memory-banks, that is, one memory-bank not precisely copying the configuration of the other due to manufacturing inaccuracy. These small errors can accumulate as the copying process is being repeated, resulting in increasing deviations from the initial path and an unreliable system. As long as the manufacturing inaccuracy does not exceed the size of a discrete interval, with discrete locking, these small errors are automatically corrected as the memory-banks copy each other's discrete configuration exactly. For similar reasons, a few decades ago, the recording of video and sound switched from analog to digital as the latter proved to be much more resilient to the corruption of information.

Conclusion

In this article, we introduced a new AM mechanism for controlling FTL propagation of a flexible cable-driven shaft. This mechanism was successfully incorporated in a prototype called Memo*Slide*, including a discrete instead of a continuous locking mechanism, making it resilient against manufacturing inaccuracies or external disturbance forces. Tests have proven the mechanism to work well, being able to transfer any path initiated by the user along the body of the mechanism without error. The Memo*Slide* is, to our knowledge, the first fully mechanical control mechanism suited for FTL propagation. Compared to a motor-driven instrument, it does not require sensors and actuators, overall resulting in a less complex and mechanically more robust control system. The Memo*Slide* sets the basis for a new direction in the development of snake-like surgical instrumentation, with a novel mechanical approach that opens new design pathways for MIS through compact anatomic environments.

Acknowledgements

The authors would like to thank technician David Jager from the DEMO Central Workshop of Delft University of Technology for the fabrication of the prototype.

Declaration of conflicting interests

The author(s) declared no potential conflicts of interest with respect to the research, authorship, and/or publication of this article.

Funding

The author(s) disclosed receipt of the following financial support for the research, authorship, and/or publication of this article: This work has been supported by the Dutch Technology Foundation STW, which is part of the Netherlands Organization for Scientific Research (NWO), and which is partly funded by the Ministry of Economic Affairs (STW Project 12137).

References

1. Roumm AR, Pizzi L, Goldfarb NI, et al. Minimally invasive: minimally reimbursed? An examination of six laparoscopic surgical procedures. *Surg Innov* 2005; 12: 261–287.
2. Targarona EM, Balague C, Knook MM, et al. Laparoscopic surgery and surgical infection. *Br J Surg* 2000; 87: 536–544.
3. Dedemadi G, Sgourakis G, Karaliotas C, et al. Comparison of laparoscopic and open tension-free repair of recurrent inguinal hernias: a prospective randomized study. *Surg Endosc* 2006; 20: 1099–1104.
4. Noguera Aguilar JF, Moreno Sanz C, Cuadrado García A, et al. NOTES. Historia v situación actual de la cirugía endoscópica por orificios naturales en nuestro país. *Cir Españ* 2010; 88: 222–227.
5. Shrestha BM. Natural orifice transluminal endoscopic surgery (NOTES): an emerging technique in surgery. *J Nepal Med Assoc* 2011; 51: 209–212.
6. Fan C, Jelinek F, Dodou D, et al. Control devices and steering strategies in pathway surgery. *J Surg Res* 2015; 193: 543–553.
7. Arkenbout E, Henselmans PJ, Jelínek F, et al. A state of the art review and categorization of multi-branched instruments for NOTES and SILS. *Surg Endosc* 2015; 29: 1281–1296.
8. Fan C, Dodou D and Breedveld P. Review of manual control methods for handheld maneuverable instruments. *Minim Invasive Ther Allied Technol* 2013; 22: 127–135.
9. Webster Iii RJ, Romano JM and Cowan NJ. Mechanics of precurved-tube continuum robots. *IEEE T Robot* 2009; 25: 67–78.
10. Gilbert HB, Rucker DC and Webster RJIII. Concentric tube robots: the state of the art and future directions. In: Inaba M and Corke P (eds) *Robotics research*. New York: Springer, 2016, pp.253–269.
11. Wu K, Wu L and Ren H. Motion planning of continuum tubular robots based on centerlines extracted from statistical atlas. In: *2015 IEEE/RSJ international conference on intelligent robots and systems*, Hamburg, 28 September–2 October 2015, pp.5512–5517. New York: IEEE.
12. Dupont PE, Lock J, Itkowitz B, et al. Design and control of concentric-tube robots. *IEEE T Robot* 2010; 26: 209–225.
13. Gilbert HB and Webster RJ. Can concentric tube robots follow the leader? In: *2013 IEEE international conference on robotics and automation*, Karlsruhe, 6–10 May 2013, pp.4881–4887. New York: IEEE.
14. Gilbert HB, Neimat J and Webster RJ. Concentric tube robots as steerable needles: achieving follow-the-leader deployment. *IEEE T Robot* 2015; 31: 246–258.
15. Waye JD. Quo vadis: another new colonoscope. *Am J Gastroenterol* 2007; 102: 267–268.
16. Shang J, Noonan DP, Payne C, et al. An articulated universal joint based flexible access robot for minimally invasive surgery. In: *2011 IEEE international conference on robotics and automation*, Shanghai, China, 9–13 May 2011, pp.1147–1152. New York: IEEE.
17. Tappe S, Pohlmann J, Kotlarski J, et al. Towards a follow-the-leader control for a binary actuated hyper-redundant manipulator. In: *2015 IEEE/RSJ international conference on intelligent robots and systems*, Hamburg, 28 September–2 October 2015, pp.3195–3201. New York: IEEE.

18. Tappe S, Kotlarski J, Ortmaier T, et al. The kinematic synthesis of a spatial, hyper-redundant system based on binary electromagnetic actuators. In: *2015 6th international conference on automation, robotics and applications*, Queenstown, New Zealand, 17–19 February 2015, pp.211–216. New York: IEEE.
19. Son J, Cho CN, Kim KG, et al. A novel semi-automatic snake robot for natural orifice transluminal endoscopic surgery: preclinical tests in animal and human cadaver models (with video). *Surg Endosc* 2015; 29: 1643–1647.
20. Nguyen TD and Burgner-Kahrs J. A tendon-driven continuum robot with extensible sections. In: *2015 IEEE/RSJ international conference on intelligent robots and systems*, Hamburg, 28 September–2 October 2015, pp.2130–2135. New York: IEEE.
21. Neumann M and Burgner-Kahrs J. Considerations for follow-the-leader motion of extensible tendon-driven continuum robots. In: *2016 IEEE international conference on robotics and automation*, Stockholm, 16–21 May 2016, pp.917–923. New York: IEEE.
22. Palmer D, Cobos-Guzman S and Axinte D. Real-time method for tip following navigation of continuum snake arm robots. *Robot Auton Syst* 2014; 62: 1478–1485.
23. Prendergast JM and Rentschler ME. Towards autonomous motion control in minimally invasive robotic surgery. *Expert Rev Med Devices* 2016; 13: 741–748.
24. Motor M, www.maxonmotor.nl/maxon/view/catalog/, 2017.
25. Kang B, Kojcev R and Sinibaldi E. The first interlaced continuum robot, devised to intrinsically follow the leader. *PLoS ONE* 2016; 11: e0150278.
26. Ota T, Degani A, Schwartzman D, et al. A highly articulated robotic surgical system for minimally invasive surgery. *Ann Thorac Surg* 2009; 87: 1253–1256.
27. Rivera Serrano CM, Johnson P, Zubiate B, et al. A transoral highly flexible robot: novel technology and application. *Laryngoscope* 2012; 122: 1067–1071.
28. Breedveld P, Sheltes JS, Blom EM, et al. A new, easily miniaturized steerable endoscope. Squid tentacles provide inspiration for the Endo-Periscope. *IEEE Eng Med Biol Mag* 2005; 24: 40–47.
29. Madhani AJ and Salisbury JK. *Articulated surgical instrument for performing minimally invasive surgery with enhanced dexterity and sensitivity*. Patent 9510915 B2, USA, 2016.
30. Gerboni G, Henselmans PW, Arkenbout EA, et al. HelixFlex: bioinspired maneuverable instrument for skull base surgery. *Bioinspir Biomim* 2015; 10: 066013.
31. Woodley BR, Oen J, Brown A, et al. System for managing Bowden cables in articulating instruments. Patent application 20090099420 A1, USA, 2009.